Part IV

Clouds, Ionized Gas, and Particles in the Local ISM

https://doi.org/10.1017/S0252921100070895 Published online by Cambridge University Press

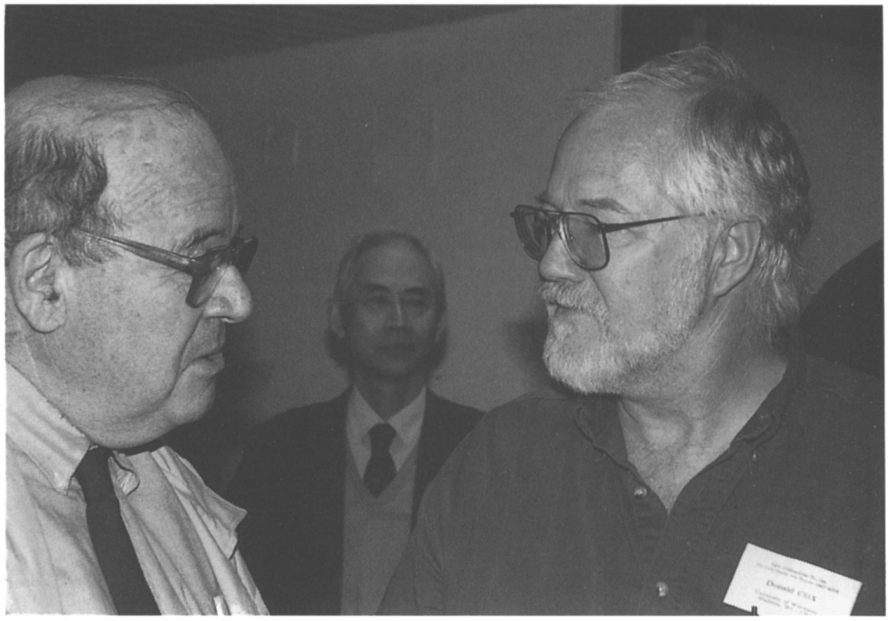

Coffee breaks with conversations ...

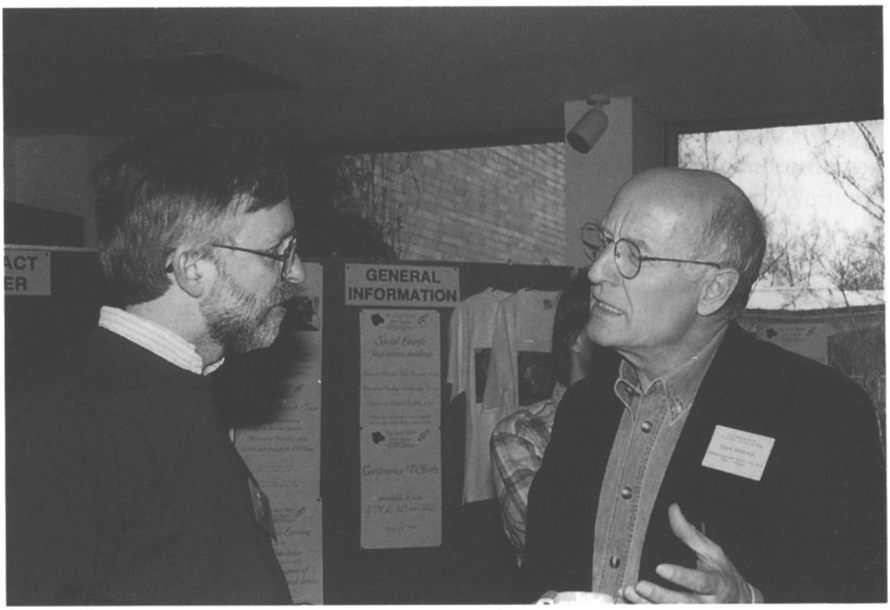

... and serious discussions.

https://doi.org/10.1017/S0252921100070895 Published online by Cambridge University Press

High-Resolution Optical Observations of Diffuse Clouds

Daniel Welty

University of Chicago, Dept. of Astronomy & Astrophysics, 5640 S. Ellis Ave., Chicago, IL 60637, USA

Abstract. We describe results from high-resolution (Δv = 0.3-1.5 km s^{-1}) observations of absorption lines due to interstellar Na I, Ca II, K I, Ca I, and Ti II. At those resolutions, we can identify and characterize many (but not all) of the individual clouds along a given line of sight; complex spatial and/or velocity structure appears to be the norm. Both the spectra and the statistics of individual cloud properties derived from fits to the observed line profiles suggest that: 1) the five species are not entirely coextensive in the neutral ISM; 2) the typical separation between adjacent components (in Na I and Ca II) is $\sim$1.2 km s^{-1}; 3) the median line widths (FWHM) for components in Na I, K I, and Ca I are $\lesssim$1.2 km s^{-1}; 4) larger line widths for Ca II, even for "corresponding" components at similar velocities, suggest that Ca II is more widely distributed; 5) line widths for clouds in the Galactic halo and in the local ISM (within 100 pc) are generally somewhat larger than for clouds in the general Galactic disk; and 6) components with very different properties (line width, relative abundances, overall column densities) are often separated by only several km s^{-1}. Observations of multiple systems and lines of sight in restricted regions reveal complex spatial structure and velocity coincidences even within 100 pc. These high-resolution optical spectra can be used to model lower resolution UV spectra of many other neutral and singly ionized species, enabling abundances and physical properties to be derived for individual interstellar clouds.

1 Introduction

One of the goals of studies of the interstellar medium (ISM) is the determination of the physical properties of the *individual* clouds which constitute the neutral component of the ISM — their temperatures, densities, relative abundances, electron fractions, internal turbulent motions, and structures — and how those properties differ for clouds in different environments. Accurate estimates of these quantities, for a significant set of individual interstellar (IS) clouds, are required to test any fundamental, global model of the ISM. Determination of individual cloud properties requires both high spectral resolution and access to the satellite UV, where the resonance lines of many important species are found. Systematic high-resolution observations of optical IS absorption lines were pioneered by Hobbs and collaborators starting nearly 30 years ago (e.g., Hobbs 1969; Marschall & Hobbs 1972; Hobbs 1984; see also Blades, Wynne-Jones, & Wayte 1980). Meyer (1994) has summarized some

https://doi.org/10.1017/S0252921100070895 Published online by Cambridge University Press

of the more recent moderate-to-high resolution optical and UV absorption-line studies of the ISM; Savage & Sembach (1996) have reviewed analyses of UV spectra obtained with the *HST* Goddard High-Resolution Spectrograph (GHRS; Δv $\sim$ 3.5 km s^{-1} for the echelle modes). In this contribution, we describe results obtained from recent very high resolution (Δv = 0.3-1.5 km s^{-1}) observations of optical absorption lines due to IS Na I, Ca II, K I, Ca I, and Ti II toward stars (mostly) within 500 pc. As will be apparent, such high resolution is necessary to discern and characterize the individual IS clouds present along many lines of sight — e.g., to distinguish clouds associated with the Local Bubble from more distant clouds. High-resolution optical spectra are thus useful for interpreting lower resolution UV spectra obtained, e.g., with the GHRS — to obtain detailed abundances and physical properties for individual IS clouds, instead of line-of-sight or component blend averages.

2 Methodology and Goals

Figure 1 shows representative spectra of various IS absorption lines toward the bright B0 Ia star ϵ Ori, obtained with the coudé spectrograph on the McDonald Observatory 2.7m (Tull 1972), the Ultra-High Resolution Facility (UHRF) on the AAT (Diego et al. 1995), and the coudé feed and 2.1m echelle spectrograph at Kitt Peak. We use the method of profile fitting to determine column densities (N), line widths ($b \sim$ FWHM/1.665), and velocities (v) for the discernible individual components (which we assume correspond to distinct IS clouds) contributing to the observed profiles. Surveys of Na I (38 stars; Welty, Hobbs, & Kulkarni 1994) and Ca II (44 stars; Welty, Morton, & Hobbs 1996) have provided new information on the statistical properties of individual IS clouds:

- Distributions of individual cloud properties (N, b, v)
- Relationships among parameters (N vs. b, b_X vs. b_Y, N_X/N_Y vs. b)
- Limits on temperature (T) and turbulence (v_t) from line widths
- Information on cloud structure from comparisons of different species
- Suggestions of environmental and/or regional differences

By combining the high-resolution optical spectra with UV spectra from GHRS (Fitzpatrick & Spitzer 1997; Welty et al. 1997a), one can undertake detailed studies of individual lines of sight sampling diverse IS environments:

- Use the high-resolution optical spectra to model the UV spectra
- Determine detailed abundance/depletion patterns for individual clouds
- Determine local physical conditions (T, n_H, n_e) for individual clouds
- Compare depletions with local physical conditions

High-resolution optical spectra are also being used to study small-scale spatial structure in the ISM (Watson & Meyer 1996) and to identify, delineate, and characterize individual clouds in the local ISM (Crawford, Craig, &

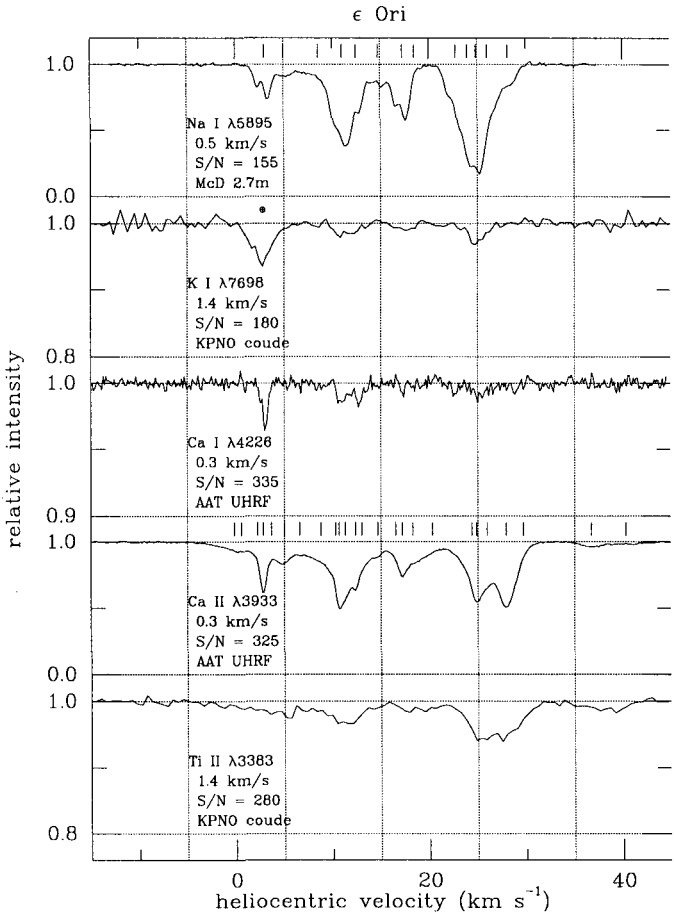

Fig. 1. High-resolution spectra of IS lines toward ϵ Ori. The resolution, S/N ratio, and source of each spectrum is indicated. Note the expanded vertical scale for K I, Ca I, and Ti II. Note also the resolved hyperfine structure in the narrowest Na I components (e.g., at 3 km s^{-1}). Tick marks above Na I and Ca II indicate components identified in fitting the profiles; 25 components (at least) are required for Ca II. Component-to-component differences in relative abundance and line width are evident.

Welsh 1997). While we focus in this contribution on high-resolution spectra of atomic species in diffuse clouds, we note that similar spectra of CH, CH^+, CN, and C_2 are allowing more detailed, component-by-component comparisons of molecular column densities, line widths, and velocities — thus providing more stringent constraints on the chemical processes operating in somewhat thicker IS clouds (e.g., Crane, Lambert, & Sheffer 1995; Crawford 1995; Sembach, Danks, & Lambert 1996).

https://doi.org/10.1017/S0252921100070895 Published online by Cambridge University Press

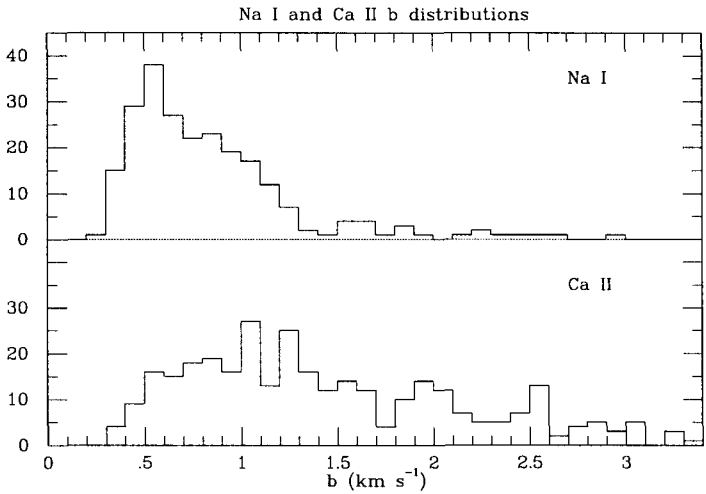

Fig. 2. Distribution of line width b ($\sim$ FWHM/1.665) for individual components in the Na I (upper) and Ca II (lower) surveys.

3 Temperature, Turbulence, and Cloud Structure

Measurements of individual component line widths, for a given species with atomic weight m, yield upper limits on the temperature and turbulence in the corresponding IS clouds, since $b = [(2kT/m) + 2v_t{}^2]^{1/2}$. If two species of significantly different m (e.g., Ca II and Na I) coexist in the same volume of gas, comparison of the widths of their corresponding components can allow estimates of the relative contributions of thermal and turbulent broadening. Comparison of the component widths for two species of similar atomic weight (e.g., Ca II and K I), on the other hand, can provide some indication of their relative spatial distribution. For example, if the widths of corresponding Ca II and K I components at the same velocity are different, then the two species cannot be identically distributed.

Figure 2 shows the distribution of b for the individual components seen in Na I (Welty et al. 1994) and Ca II (Welty et al. 1996). Even though the lines of sight sampled in the two surveys are very similar, the median b-values differ significantly: 0.73 km s^{-1} for Na I and 1.31 km s^{-1} for Ca II. Preliminary results for K I and Ca I suggest median b-values of about 0.65-0.70 km s^{-1} for both species. For all four species, the smallest b-values measured are in the range 0.3-0.4 km s^{-1}. Since the thermal contribution to the b-values, for $T = 100$ K, is 0.27 km s^{-1} for Na I and 0.21 km s^{-1} for Ca II, K I, and Ca I, the observed minimum and median b-values suggest either that the cloud temperatures are higher, that there is a significant turbulent contribution to the line widths, and/or that most narrow lines are obscured by blending. If 80 K is a representative temperature for the clouds detected in Na I, then at

least 38% (and perhaps the majority) of those clouds have subsonic internal turbulent motions [assuming an isothermal sound speed $v_s \sim 0.7(T/80\ \mathrm{K})$]. If most of the gas traced by Ca II absorption is warmer than about 400 K, then the turbulence in that gas would also be subsonic.

Different subsets of the Na I and Ca II component samples can have different b-value distributions. Ca II components observed toward stars in the Galactic halo and components seen only in Ca II toward disk stars both have very broad distributions, with $b_{\mathrm{med}} \sim 1.6$-$1.7$ km s^{-1}. Ca II components found within 100 pc are on average somewhat broader, with $b_{\mathrm{med}} \sim 2.1$ km s^{-1} (e.g., Crawford et al. 1997). That median value is consistent with the $T \sim 6000$-7000 K and $v_t \sim 1$ km s^{-1} derived from UV spectra of very nearby clouds (Piskunov et al. 1997). There are, however, some cold components, with $b \lesssim 0.5$ km s^{-1}, both in the Galactic halo (e.g., Pettini 1988) and in the local ISM within 50 pc (Welty et al. 1994, 1996; Jenkins 1997).

Given the definition of the line-width parameter b, we would expect, if Ca II and Na I are similarly distributed, that $0.76 \leq b(\mathrm{Ca\ II})/b(\mathrm{Na\ I}) \leq 1.0$, where the lower limit corresponds to purely thermal broadening and the upper limit to purely turbulent broadening. From the Na I and Ca II surveys, we have identified 72 "corresponding" components for which the velocities agree to within 0.2 km s^{-1} and for which any significant near neighbor components also have similar velocities for both species. Contrary to the above expectation, b(Ca II) is often *greater* than b(Na I) for the individual corresponding components; the median b-values for the sub-sample of 53 best-determined corresponding components are 0.84 and 0.65 km s^{-1} for Ca II and Na I, respectively. The most straightforward explanation for this difference in b-values is that Ca II and Na I are not identically distributed, even though similar component velocities suggest they are associated (see also Blades et al. 1997). For a given velocity component, Ca II probably occupies a somewhat larger volume, characterized by a larger temperature and/or greater turbulence, than does Na I — likely related to enhanced grain erosion (and thus less severe Ca depletion) in the warmer, more diffuse gas outside the cloud cores (Barlow et al. 1995).

Detailed component-by-component comparisons of high-resolution spectra of Ca II, Na I, K I, Ca I, and Ti II provide additional insight into the structure of neutral IS clouds. The five species are characterized by different ionization and depletion behavior, and as a result appear to be distributed somewhat differently. Comparisons of high-resolution Ca II and Ti II spectra seem to show detailed correspondence in velocity and relative column density in many cases (Welty, Lauroesch, & Fowler 1997), consistent with a suggestion that Ca II and Ti II are often found in warm, diffuse gas, where both Ca and Ti are much less depleted than in cold, dense clouds (Crinklaw, Federman, & Joseph 1994; see also Stokes 1978). In such warm, diffuse H I gas, Ca II ($\chi_{\mathrm{ion}} \sim 11.9$ eV) is presumably a trace ionization state, while Ti II ($\chi_{\mathrm{ion}} \sim 13.6$ eV) is dominant. We note, however, that the observed line

widths imply that at most 40% of the Ca II components could arise in gas with $T \gtrsim 6000$ K. In addition, there are relatively narrow Ca II components that correspond to narrow components seen in Na I and K I, for which Ti II is not similarly enhanced (see Fig. 1). The strong, narrow components in Na I and K I presumably arise primarily in the colder, denser cloud cores, since as trace ionization states their abundances should be proportional to $n_{\rm H}^2$. The Ca I absorption detected for some of those lines of sight also appears to arise in those narrow components (Welty, Hobbs, & Morton 1997), and the Ca I/Ca II ratio suggests that Ca II is the dominant form of Ca there. Apparently the transition of Ca II from a trace to a dominant species can substantially offset the strong depletion of Ca in the denser cloud cores. The interplay between two strongly variable effects — the Ca depletion and the Ca II–Ca III ionization balance — may explain the otherwise surprising similarity between the Ca II profiles and the profiles of other singly ionized species such as Zn II, Si II, and Fe II (which are typically dominant ionization stages in both warm and cold H I regions) seen in GHRS echelle spectra.

4 Complex Velocity and Spatial Structure

Examination of individual high-resolution, high S/N ratio spectra (e.g., Fig. 1) indicates that the component structures can be very complex. Furthermore, when the Ca II component structures are compared with those derived independently for Na I for the same lines of sight, we find that while a number of components do show good correspondence, there are also many which do not line up — which may indicate unresolved structure in one or both of the species. If the component velocities for the true complete sample of clouds (for either Ca II or Na I) are both uncorrelated and taken from a single Poisson distribution, then the distribution of velocity separations (δv) between adjacent components will be an exponential function of δv: $\ln[{\rm N}(\delta v)] = \alpha + \beta \times \delta v$. Figure 3 shows that the δv distributions are well-fitted by exponentials (with very similar slopes) at intermediate δv, as would be expected for uncorrelated component velocities. The slight excesses over the fits at higher δv are likely due to a population of higher velocity clouds. The fall-offs at small δv, however, suggest that unresolved component structure is present, even in these very high-resolution (Δv = 0.3-1.2 km s^{-1}) spectra. Extrapolations of the fits to $\delta v = 0$ suggest that we have discerned only about 60% and 40% of the true number of Na I and Ca II components, respectively, and that the true median δv for both species is about 1.2 km s^{-1}. We see no evidence for any non-random, preferential clumping of components, which would cause a steepening of the δv distributions, at least for $\delta v \gtrsim$ 1-2 km s^{-1}.

High-resolution spectra of Na I and Ca II have also revealed indications of significant small-scale spatial structure in the ISM. Meyer & Blades (1996) presented UHRF spectra of Na I and Ca II toward both members of the binary μ Cru, which has a projected separation of 6600 AU at a distance

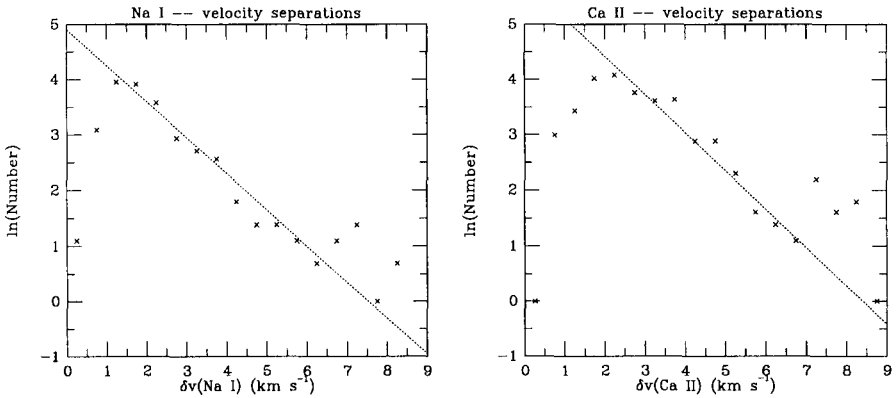

Fig. 3. Distribution of adjacent component separations [ln $N(\delta v)$] for the Na I (left) and Ca II (right) surveys. Dotted lines indicate linear fits for intermediate values of δv [corresponding to exponential fit to $N(\delta v)$].

of 170 pc. They found dramatic differences in N(Na I) (factors $\gtrsim 4$) for three of the seven components in the Na I profiles, with corresponding (but smaller) differences for Ca II. In Na I spectra obtained at a resolution of 1.4 km s^{-1}, Watson & Meyer (1996) found differences in the line profiles for *all* of the 17 multiple systems observed, with projected separations of 500-30,000 AU. [By contrast, earlier lower resolution Ca II spectra of 12 binary systems had revealed only several cases with significant differences (Meyer 1994).] The differences seem to be most pronounced for Na I, and in particular for the narrowest components and/or those with higher Na I/Ca II ratios — consistent with the picture of cloud structure and species distribution discussed above. The differences in N(Na I) imply density contrasts of order 10^3 cm^{-3} — similar to those determined for the small (5-100 AU) neutral clouds inferred in several 21 cm studies (e.g., Frail et al. 1994). This apparently pervasive structure may be due to very cold ($T \sim 15$ K), dense filaments or sheets, embedded in warmer, less dense neutral gas and containing 10-30% of the total column density of cold, neutral gas (Heiles 1997).

The complex velocity structure found along many lines of sight and the small-scale spatial structure observed over small angular scales suggests that determining the detailed three-dimensional structure of the cold, neutral component of the ISM will be very difficult. Mapping the warmer, presumably more smoothly distributed material in the local ISM should be more feasible, but will still require sensitive, high resolution observations of many stars with well determined distances. High-resolution Ca II spectra of stars within 50 pc have revealed multiple components and velocity coincidences (i.e., components with similar velocities but different distances along a given line of sight) even within that restricted volume (Crawford & Dunkin 1995; Crawford et al. 1997; Welsh, Crawford & Lallement 1997; Frisch & Welty 1997).

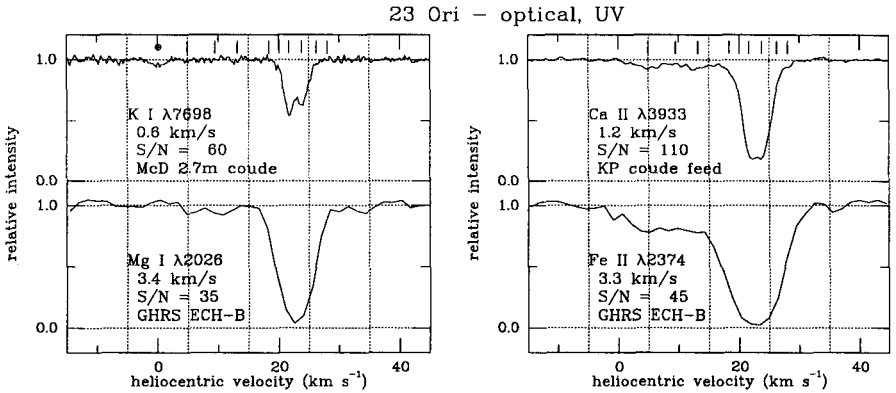

Fig. 4. Detailed component structure (tick marks) seen in high-resolution optical K I and Ca II spectra of 23 Ori cannot be discerned in lower resolution UV spectra of Mg I and Fe II obtained with GHRS. The optical data can be used to model the UV lines, however, to obtain detailed abundances and physical conditions for individual clouds.

5 Abundances, Depletions, and Physical Conditions

The statistics of component line widths and adjacent component separations imply that, for many lines of sight, much of the component structure will not be discernible, and many individual components will not be resolved, in UV spectra obtained with GHRS or STIS. Furthermore, the high-resolution optical spectra show that components with very different properties (e.g., overall column densities, line widths, Na I/Ca II ratios) are often separated by only several km s^{-1} along a given line of sight. Fortunately, however, the high-resolution optical spectra can be used to model the lower resolution UV spectra, so that abundances and physical conditions can be derived for individual IS clouds from the transitions observed in the UV spectra.

Figure 4 shows high-resolution optical spectra of K I and Ca II (upper) and GHRS echelle spectra of Mg I and Fe II (lower) observed toward the B1 V star 23 Ori (Welty et al. 1997a). Profile analysis of the high-resolution optical spectra of Na I, K I, Ca I, and Ca II indicates that the absorption near +22 km s^{-1} is due to two main components, separated by about 2.1 km s^{-1}, plus several weaker outlying components. The apparent similarity in b-values for the two strong components in Na I and K I suggests that the gas is cold, with the line widths dominated by turbulent broadening. For those two strongest components, the column densities for K I, Ca II, and Ca I can be used, together with the equation of ionization equilibrium, to estimate both the relative n_e and the relative column densities of many other neutral and singly ionized species observed (but not resolved) in the UV spectra. The absorption seen between 0 and +15 km s^{-1} is due to at least three weaker, somewhat broader components — probably warmer, lower density

https://doi.org/10.1017/S0252921100070895 Published online by Cambridge University Press

gas. Application of this component structure model to the GHRS echelle spectra yields individual component column densities for Zn II, Fe II, Si II, Cr II, Ni II, Mg I, S I, Si I, and Fe I, with formal uncertainties typically ±0.1 dex or better. For several neutral–first ion pairs in the two strong components, we find $n_e \sim 0.06 \pm 0.03$ cm^{-3}, assuming $T \sim 100$ K (from *Copernicus* H_2 data) and photoionization by the "typical" IS radiation field. Analysis of the C I fine structure excitation (Jenkins & Shaya 1979) yields a pressure $\log(n_H T) \sim 3.1$ cm^{-3}K, and thus $n_H \sim$ 10-15 cm^{-3} (for $T = 100$ K) and a total thickness of about 12-16 pc for the two main clouds. The fractional ionization $n_e/n_H \sim 5 \times 10^{-3}$ implied for those two clouds is a factor ~ 15 larger than expected from photoionization of heavy elements. If N(Zn II) is used to infer N(H) for the individual components, we can examine the depletions of different elements in the various components. The depletions in the components at 0 to +15 km s^{-1} are similar to those found for warm, low density gas. It is intriguing that the two strongest components toward 23 Ori have both lower n_H and less severe depletions than the main component(s) observed toward ζ Oph (Savage, Cardelli, & Sofia 1992). Analyses of additional lines of sight will be needed to test any possible general relationship between n_H and depletion — and thus to constrain the processes giving rise to the observed depletions.

Fitzpatrick & Spitzer (1997) have performed a detailed study of the line of sight to the halo star HD 215733, using high-resolution Ca II and H I data to help interpret GHRS echelle spectra of many other species. They find 23 neutral (H I) components between −95 and +15 km s^{-1}, with b(heavy elements) ranging from 0.5-6.6 km s^{-1}, log[N(H)] from 17.5-20.1 cm^{-2}, and T from $\lesssim 200$ K to $\gtrsim 1000$ K. The depletion of Fe is always at least a factor of 4, even at $|v_{LSR}| \gtrsim 50$ km s^{-1}. Estimates of n_e based on the ionization equilibria of C, Mg, S, and Ca appear to differ systematically, perhaps due to charge exchange or other processes; n_e/n_H in several cold clouds may be consistent with the electrons coming from photoionization of heavy elements.

We conclude with a few observations noted in comparing various quantities (individual component or integrated line-of-sight values):

- N and b show no obvious correlation, for either Na I or Ca II.
- Na I/Ca II shows a wide range for any $b \lesssim 1.5$ km s^{-1}, and Na I/Ca II $\lesssim 1.0$ can occur for a wide range of b (e.g., even in gas with $T \lesssim 1000$ K).
- Na I and H I may be reasonably well correlated for N(Na I) $\gtrsim 10^{11}$ cm^{-2}, but not for lower N(Na I).
- Ca I/Ca II shows little, if any variation with f(H_2) (fraction of H in molecular form, which should depend on n_H and radiation field). Does n_e not depend on n_H?
- Electron densities calculated from Ca I/Ca II, and depletions of Na, K, and Li inferred from those n_e, may be systematically in error.

Acknowledgements. The following have participated in the acquisition and/or analysis of the high-resolution spectra discussed above: L. Hobbs, D. Morton, P.

Frisch, V. Kulkarni, J. Lauroesch, J. Fowler, E. Fitzpatrick, M. Lemoine, J. Trapero. We appreciate the assistance of D. Doss (McDonald), J. Spyromilio and S. Ryan (AAO), and D. Willmarth (KPNO) in obtaining the spectra. We gratefully acknowledge support from NASA grant NAG5-3228.

References

Barlow, M. J., Crawford, I. A., Diego, F., Dryburgh, M., Fish, A. C., Howarth, I. A., Spyromilio, J., & Walker, D. D. (1995): MNRAS 272, 333
Blades, J. C., Sahu, M. S., He, L., Crawford, I. A., Barlow, M. J., & Diego, F. (1997): ApJ 478, 648
Blades, J. C., Wynne-Jones, I., & Wayte, R. C. (1980): MNRAS 193, 849
Crane, P., Lambert, D. L., & Sheffer, Y. (1995): ApJS 99, 107
Crawford, I. A. (1995): MNRAS 277, 458
Crawford, I. A., Craig, N., & Welsh, B. Y. (1997): A&A 317, 889
Crawford, I. A. & Dunkin, S. K. (1995): MNRAS 273, 219
Crinklaw, G., Federman, S. R., & Joseph, C. L. (1994): ApJ 424, 748
Diego, F. et al. (1995): MNRAS 272, 323
Fitzpatrick, E. L. & Spitzer, L. (1997): ApJ 475, 623
Frail, D. A., Weisberg, J. M., Cordes, J. M., & Mathers, C. (1994): ApJ 436, 144
Frisch, P. C. & Welty, D. E. (1997): in preparation
Heiles, C. (1997): ApJ 481, 193
Hobbs, L. M. (1969): ApJ 157, 135
Hobbs, L. M. (1984): ApJS 56, 315
Jenkins, E. B. (1997): these proceedings
Jenkins, E. B. & Shaya, E. J. (1979): ApJ 231, 55
Marschall, L. A. & Hobbs, L. M. (1972): ApJ 173, 43
Meyer, D. M. (1994): in The First Symposium on the Infrared Cirrus and Diffuse Interstellar Clouds, ed. R. M. Cutri & W. B. Latter (San Francisco: PASP), 3
Meyer, D. M. & Blades, J. C. (1996): ApJ 464, L179
Pettini, M. (1988): Proc. Astron. Soc. Aust. 7, 527
Piskunov, N., Wood, B. E., Linsky, J. L., Dempsey, R. C., & Ayres, T. R. (1997): ApJ 474, 315
Savage, B. D., Cardelli, J. A., & Sofia, U. J. (1992): ApJ 430, 650
Savage, B. D. & Sembach, K. R. (1996): ARA&A 34, 279
Sembach, K. R., Danks, A. C., & Lambert, D. L. (1996): ApJ 460, L61
Stokes, G. M. (1978): ApJS 36, 115
Tull, R. G. (1972): in Proc. ESO/CERN Conference on Auxiliary Instrumentation for Large Telescopes (Geneva: ESO), 259
Watson, J. K. & Meyer, D. M. (1996): ApJ 473, L127
Welsh, B. Y., Crawford, I. A., & Lallement, R. (1997): these proceedings
Welty, D. E., Hobbs, L. M., & Kulkarni, V. P. (1994): ApJ 436, 152
Welty, D. E., Hobbs, L. M., Lauroesch, J. T., Morton, D. C., Spitzer, L., & York, D. G. (1997a): in preparation
Welty, D. E., Hobbs, L. M., & Morton, D. C. (1997b): in preparation
Welty, D. E., Lauroesch, J. T., & Fowler, J. R. (1997c): in preparation
Welty, D. E., Morton, D. C., & Hobbs, L. M. (1996): ApJS 106, 533